Biotechnology and Bioprocess Engineering
DOI 10.1007/s12257-021-0133-y

pISSN 1226-8372
eISSN 1976-3816

RESEARCH PAPER

Carboxylesterase3 (Ces3) Interacts with Bone Morphogenetic Protein 11 and Promotes Differentiation of Osteoblasts via Smad1/5/9 Pathway

Sulagna Mukherjee, Jong Pil Park, and Jong Won Yun

Received: 14 May 2021 / Revised: 6 June 2021 / Accepted: 8 June 2021

Abstract Ces3 is a lipolytic enzyme predominantly present in liver and adipocytes, with recent reports of its presence in skeletal muscles, as well. A cross-linking study to understand the various interacting proteins involved in bone-adipose axis could provide novel targets for drug development. We explored the functional role of Ces3 in osteoblasts and mesenchymal stem cells differentiating into osteoblast lineage using *in vitro* models. We also investigated the physiological functions of Ces3 by stable gene knockdown of *Ces3* and exogenous Ces3 induction, and examined the interacting proteins by Co-IP and *in-silico* analysis. Data from our study suggests that *Ces3* is highly expressed in osteoblasts and promotes proliferation of the cells by increasing the expressions of osteogenic marker proteins and genes. For the first time, our mechanistic studies revealed that Ces3 interacts with BMP11 protein for regulation of osteoblast differentiation and activates the ALK2 and BMP type II receptors via Smad 1/5/9 signaling pathways. In addition, we identified the various partner proteins linked to Ces3 and BMP11 which are also involved in the metabolic network of osteoblasts. *In silico* analysis revealed a direct and strong interaction between Ces3 and BMP11 which influences the growth and regulation of osteoblasts. Current data unveiled a hitherto unknown mechanism of Ces3 and BMP11 in the bone-adipose axis, shedding light on Ces3 as a pharmaco-therapeutic target to treat metabolic disorders.

Sulagna Mukherjee, Jong Won Yun*
Department of Biotechnology, Daegu University, Gyeongsan 38453, Korea
Fax: +82-53-850-6559
E-mail: jwyun@daegu.ac.kr

Jong Pil Park
Department of Food Science and Technology, Chung-Ang University, Anseong 17546, Korea

Keywords: osteoblasts, Ces3, BMP11, differentiation, Smad 1/5/9

1. Introduction

The bone has emerged as an endocrine organ with effects on body weight control and glucose homeostasis through the actions of several bone-derived factors. The cross-talk between adipose tissue and the bone constitutes a homeostatic feedback system with adipokines and molecules secreted by osteoblasts and osteoclasts representing the links of an active bone-adipose axis [1]. Several diseases including type 2 diabetes mellitus and osteoporosis are reported to be correlated with the fat-bone relationship [2], but the balanced metabolism with reduced fat accumulation and increased osteoblast differentiation resulted in effective way to combat the diseases [3]. Osteoblasts are the primary cells involved in osteogenic differentiation [4], while the pluripotent mesenchymal stem cells (MSCs) have the ability to transform into osteoblasts as well as adipocytes [5]. The differentiation of osteoblastogenic and adipogenic programs are well coordinated and established in a competitive manner [6]. The cell lineages of adipocytes and osteoblasts share a degree of plasticity and several regulators contribute to control their differentiation and function [7]. Among the known transcriptional factors responsible for osteoblast differentiation, Runt-related transcription factor 2 (Runx2), alkaline phosphatase (ALP) and Osterix (Osx) are modulated via phosphorylation of Smad 1/5/9 and play vital roles in the formation of the bone matrix [8,9].

The bone morphogenetic protein 11 (BMP11), also known as growth and differentiation factor 11 (GDF11) [10], is a protein known to play a role in bone formation. BMP11 belongs to the superfamily of transforming growth factor-

β (TGF-β) proteins [11], and has been implicated in several diseases including cancer [12], aging [13], obesity, and diabetes [14]. Interestingly, in our recent study we have highlighted the unique role of BMP11 regulating thermogenesis in white fat cells [15]. BMP11 has also been linked with adipocyte lipolytic protein carboxylesterase 3 (Ces3 for rodents, CES3 for humans) in the regulation of skeletal muscle [16].

Ces3, also known as Ces1d, belongs to the multigene superfamily of enzymes responsible for catalyzing long and short-chain glycerol, amide bonds and hydrolyzing esters [17]. Other predominant functions include bioconversion of prodrugs [18], and detoxification of drugs and xenobiotics [19,20]. Among all the other isoforms [21], Ces3 is reported as an important adipocyte lipase [22,23], and considered as a triglycerol hydrolase (TGH) [24]. Previous studies have demonstrated that loss of Ces3 impairs glucose metabolism through accumulation of excess lipid and diminishing mobility of cholesterol esters [25,26]. Other studies suggest a role for Ces3 in the regulation of obesity [27], steatosis, and hyperlipidemia [28,29]. The functional role of Ces3 in adipogenesis, however, remains controversial [30]. For example, studies have reported that Ces3 down-regulates PPARγ signaling [31,32]. In our previous studies, we established a significant role of Ces3, as well as BMP11 in the regulation of white adipocytes by promoting browning of white fat and energy homeostasis via mitochondrial thermogenesis [33,15].

However, there are no reports on the physiological role of Ces3 in bone. Therefore, in this study, we investigated the effects of Ces3 in osteoblasts and mesenchymal stem cells to elucidate the metabolic events regulated by Ces3. This is the first report to identify the presence of Ces3 in osteoblasts and its relation with other bone proteins involved in the differentiation and proliferation of osteoblasts into osteocytes, as well as role of BMP11 in regulating osteodifferentiation.

2. Materials and Methods

2.1. Chemicals

LDN193189 (antagonist of ALK2/3) was purchased from AdooQ (Irvine, CA, USA). Other chemicals used were of analytical grade.

2.2. Cell culture and differentiation

The preosteoblasts MC-3T3-E1 cells (ATCC, Manassas, VA, USA) were cultured in α-minimal essential medium (α-MEM) (Gibco, Thermo Fisher Scientific Corp., Waltham, MA, USA) without ascorbic acid, supplemented with 10% fetal bovine serum (FBS, PAA Laboratories, Pashing, Austria) at 37°C in a 5% CO_2 incubator. The C3H10T1/2 mesenchymal stem cells were maintained in high glucose Dulbecco's Modified Eagle's Medium (DMEM, Thermo, Waltham, MA, USA) supplemented with 10% fetal bovine serum (FBS, PAA Laboratories, Pasching, Austria) at 37°C in a 5% CO_2 incubator. For osteogenic differentiation, the cells were cultured with osteogenic medium, α-MEM containing 50 μg/mL of ascorbic acid and 5 mM of β-glycerophosphate for 10-20 days.

2.3. Subcellular fractionation

The 100% confluent preosteoblasts cells were subjected to osteogenic media and cultured for 10-12 days (with change of media every 2/3 days). Freshly scrapped cells were used for subcellular fractionation following the protocol reported by Dimauro *et al*. (2012) [34]. The fractionation of the samples were validated by western blotting.

2.4. Real-time qRT-PCR

Total RNA was extracted from cells using the total RNA isolation kit (RNA-spin, iNtRON Biotechnology, Seongnam, Korea) according to the manufacturer's instructions. The quantitative and qualitative ratio metric analysis of RNA was performed using a microplate reader (Tecan Infinite

Table 1. List of primers used for real-time qRT-PCR

Gene	Forward	Reverse
Acvr1	ATGGTAGTCGTCCAAGGAGC	GGCTTGGCTTTACACAGACG
Acvr2a	TGGTCCCATGAACTTGCACT	GGGTCAGAAGCGATGTTTTCA
Acvr2b	AGGCCTCTCTCTCATCGTCC	AGGCAAGGGCTTAAAGGAGTC
Alp	GGGCCTGCTCTGTTTCTTCA	CTGAGATTCGTCCCTCGCTG
Bmp11	AACCATACCTCAGCAGTGGC	CGGTCAGGCTTCAGTTCAGT
Bmpr2	AGGCTTGCTGTAAAATGGTGC	AGTGTGTGCTGACTCTATTGC
Bglap	CCCAGACCTAGCAGACACCA	CCTGCTTGGACATGAAGGCT
Ces3	GCCAACTTTGCTCGGAATGG	GCCTGAGTTGAGGCACCAAT
Runx2	CGCCTCACAAACAACCACAG	GAGCACTCACTGACTCGGTT
Sp7	AGAGTGAGCTGGCCTGAGAGAG	CGCCATCCTCGAGCTGGGTA
Tgfβ3	GGACTTCGGCCACATCAAGA	ATAGGGGACGTGGGTCATCA

M200 Pro, Männedorf, Switzerland). cDNA was synthesized from RNA (1 μg) by applying the Maxime RT premix (iNtRON Biotechnology). Power SYBR Green (Roche Diagnostics Gmbh, Mannheim, Germany) was used to quantitatively determine the transcript levels of genes with RT-PCR (Roche LightCycler® 96). PCR reactions were run in duplicate for each sample, and transcript levels of each gene were normalized to β-actin. Table 1 lists the sequences of primer sets used in this study.

2.5. Gene silencing

Commercially available siRNA specific for *Ces3* (a pool of three target-specific 21 nucleotides siRNA designed to knockdown gene expression) and siRNA specific for *Bmp11* (Thermo Fisher Scientific Corp.) was used for gene silencing in both MC-3T3-E1 and C3H10T1/2 cells (siRNA sequences are listed in Table S1). Post confluent MC-3T3-E1 and C3H10T1/2 cells in six-well culture dishes were washed twice with transfection medium overlaid by using a previously prepared mixture of siRNA and transfection reagent (Roche Diagnostics). The transfection process was continued for 48 h in case of MC-3T3-E1 cells and 24 h for C3H10T1/2 cells, respectively, after which the differentiation medium was added. After 10 days, mature cells were collected for further experiments.

2.6. Treatment of recombinant proteins

Recombinant mouse Ces3 protein (rCes3) with a His tag with 96% purity of Ces3 was purchased from Sino Biological Inc. (Wayne, PA, USA) and recombinant BMP11 (rBMP11) protein was purchased from PreproTech (Rocky Hill, NJ, USA). MC-3T3-E1 and C3H10T1/2 cells were seeded at 0.8×10^5 cells/well in 6-well plates after trypsinization and grown to 70% and 100% confluence for one or three days, respectively, then treated with 10 ng/mL of rCes3 and 20 ng/mL of rBMP11 during differentiation for 10 days.

2.7. ALP staining

MC-3T3-E1 and C3H10T1/2 cells were cultured with silenced *Ces3* or *Bmp11*, as well as with rCES3 for 10 days and the mineralization was analyzed by ALP staining. The cultured cells were rinsed with PBS followed by fixation with 20% formalin solution for less than 2 min and then treated with a BCIP®/NBT solution (Sigma Aldrich) for 20 min. The stained cultures were visualized using an inverted microscope and the intensity of fold change was measured by using the ImageJ software (NIH).

2.8. Co-Immunoprecipitation (Co-IP)

To identify the interaction between Ces3 and BMP11 as well the interacting partner proteins, Co-IP using anti-Ces3 (Santa Cruz Biotechnology Inc., Dallas, TX, USA) and anti-BMP11 (Abcam, Cambridge, UK) were carried out according to the method outlined by Bridges *et al.* (2012) [35], followed by SDS-PAGE and silver staining. To identify the proteins by peptide mass fingerprinting, the protein bands were excised, digested with trypsin (Promega, Madison, WI), mixed with α-cyano-4-hydroxycinamic acid in 50% acetonitrile/0.1% TFA, and subjected to MALDI-TOF analysis (Microflex LRF 20, Bruker Daltonics, Billerica, MA, USA). Peak list was generated using Flex analysis 3.0, followed by protein identification using the Mascot search engine (Matrix Science Inc., Boston, MA, USA). The identified proteins were analyzed using computational tools to generate a protein interaction network.

2.9. Immunoblot analysis

Cell lysates were prepared by homogenization in RIPA buffer (Sigma) followed by centrifugation at 13,000×*g* for 30 min. Cell extracts were then diluted in 5× sample buffer (50 mM Tris at pH 6.8, 2% SDS, 10% glycerol, 5% β-mercaptoethanol, and 0.1% bromophenol blue) and heated at 95°C for 5 min before 8, 10, or 12% SDS-polyacrylamide gel electrophoresis (PAGE). Following electrophoresis, samples were transferred onto a polyvinylidene difluoride membrane (PVDF, ATTO Technology, Amherst, NY, USA) and then blocked for 1 h with TBS-T (10 mM Tris-HCl, 150 mM NaCl, and 0.1% Tween 20) containing 5% skim milk (Sigma) or BSA (Rocky Mountain Biologicals, Missoula, MT, USA). The membrane was subsequently rinsed three times consecutively with TBS-T buffer followed by incubation at room temperature for 1 h with 1:1,000 diluted primary polyclonal antibodies, including anti-ALK2, anti-ALP, anti-β-actin, anti-BMPRII, anti-Ces3, anti-OSX, anti-Smad 2/3, anti-Smad4, anti-TGFβ3 (Santa Cruz Biotechnology, Inc.), anti-p-Smad 2/3, anti-p-Smad1/5/9 (Cell Signaling Technology, Danvers, MA, USA), anti-RUNX2, anti-BMP11 (Abcam, Cambridge, UK), and anti-Smad 1/5/9 (Elabscience, Houston, TX, USA), in TBS-T buffer containing 1% skim milk or BSA. After three washes, the membrane was incubated with horseradish peroxidase-conjugated anti-goat IgG, anti-rabbit IgG or anti-mouse IgG secondary antibody (1:1000, Santa Cruz Biotechnology) in TBS-T buffer containing 1% skim milk or BSA at room temperature for 1 h. Next, immunoblots were developed with enhanced chemiluminescence and captured using an ImageQuant LAS500 system (GE Healthcare Life Sciences, Marlborough, MA, USA). Band intensities were quantified with the ImageJ software (NIH, Bethesda, MD, USA).

2.10. Immunofluorescence

Immunocytochemistry was performed on 4% formaldehyde-fixed cells. These cells were incubated with anti-Ces3 (dilution 1:1000, Santa Cruz Biotechnology) primary

antibody at 4ºC overnight followed by incubation with appropriate FITC goat anti-mouse secondary antibody at room temperature for 4 h. For staining of mitochondria, MitoTracker®Red (1 mM, Cell Signaling Technology) was directly added to PBB-T (PBS + 1% BSA and 0.1% Tween 20) at a concentration of 200 nM. Cells were then incubated at 37ºC for 2 h. After incubation, tissues were washed with PBS and subjected to immunostaining. Morphological findings were observed using a light microscope at X10 magnification.

2.11. Network analysis

Computational analysis was performed using STRING (version 11.0), a biological database and web resource of known and predicted protein-protein interactions. The threshold confidence was set between high to medium (0.700-0.150), network edges were set based on evidence, experiment and molecular interactions. Maximum number of interactors for the 1st shell with no more than 5 and for 2nd shell with no more than 10 interactions.

2.12. Molecular docking analysis

The protein targets used in this study, Ces3 (uniprot ID: Q8VCT4) and BMP11 (uniprot ID: Q9Z1W4) were selected based on the results obtained from Mascot search engine and confirmed for the isoform types in the Uniprot protein database (www.uniprot.org). The 3D structures were retrieved from the Swiss-model database (https://swissmodel.expasy.org). The structure models were refined at resolutions < 4.2 Å, with 80.60% sequence identity and 0.56 sequence similarity for Ces3 (oligo-state of homo-3-mer) and 67.47% sequence identity and 0.52 sequence similarity in case of BMP11 (oligo-state of homo-2-mer). Molecular docking was performed using the PatchDock online docking server with Beta 1.3 version. The pdb files for protein structures were uploaded to the server with default rigid molecular docking setting to generate up to 10 binding confirmations. This software uses the molecular docking algorithm based on shape complementarity principles and predicts the approximate interface area of the complex [36], as well as the atomic contact energy [37] to identify the free binding energies.

2.13. Statistical analysis

All data are presented as the means ± SD of at least three independent experiments. Statistical significance among multiple groups was determined by one-way analysis of variance (ANOVA) followed by Tukey's post-hoc test or two-tailed Student's *t*-test using the Statistical Package of Social Science (SPSS) software version 17.0 (SPSS Inc., Chicago, IL, USA). Statistical significance was indicated as either $p < 0.05$ or $p < 0.01$.

3. Results

3.1. Expression of Ces3 in osteoblasts

We examined the differentiation of osteoblasts by analyzing the expression of osteogenic differentiation marker proteins for MC-3T3-E1 cells (Fig. 1A) in a day-dependent manner and in C3H10T1/2 cells after induction of osteogenic media (Fig. S1A). The expression of all the marker proteins elevated day-dependently upto day 10, indicating successful differentiation of preosteoblasts and mesenchymal stem cells into mature osteoblasts. The expression for BMP11 and Ces3 proteins was observed to be very similar to the expression for the osteogenic differentiation marker proteins. Similarly, we determined the gene expressions of the transcription factors responsible for osteoblast differentiation such as *Runx2*, *Sp7*, and *Alp* along with *Ces3*, which showed increased expression day-dependently in MC-3T3-E1 cells (Fig. 1B) and C3H10T1/2 cells (Fig. S1A). In addition, to ascertain the location of Ces3 in osteoblast cells, we performed the subcellular fractionation for MC-3T3-E1 cells and determined the presence of Ces3 in cytosol and partly in nucleus (Fig. 1C), after comparing with the standard protein markers: β-actin (cytosol), COXIV (mitochondria) and Lamin (nuclei). Finally, to confirm our results for expression of *Ces3*, we validated the intensity of florescence at cellular level by immunocytochemistry (Fig. 1D), where the intensity of *Ces3* significantly increased at day 6 and day 10, and indicating presence of Ces3 protein in MC-3T3-E1 osteoblasts.

3.2. Ces3 promotes proliferation of osteoblasts

To study the functional role of Ces3 in osteoblasts, initially we treated the MC-3T3-E1 cells with rCes3 in a concentration-dependent manner (Fig. 2A) and optimized the concentration of 10 nM. Then, we examined the expression of osteogenic genes (Fig. 2B), which showed elevated expression levels in rCes3-treated cells. We also determined the protein markers of differentiation for osteoblasts (Fig. 2C), as well as in C3H10T1/2 cells (Fig. S1B) along with gene expressions (Fig. S1C) and observed higher expression levels in rCes3-treated cells. Next, we determined the effect of *Ces3* depletion on osteoblasts by silencing *Ces3* using transfection of the cells with 600 pM of *Ces3* siRNA. Expression of *Ces3* was significantly impeded by nearly 60% in cells transfected with siRNA targeting *Ces3*, as compared to the wild-type cells. This indicates that the knockdown cell model was successfully constructed and could be used in subsequent experiments. Remarkably, not only all the osteogenic protein markers showed reduced expression in MC-3T3-E1 cells (Fig. 2D), but also the genetic factors involved in differentiation of osteoblasts reduced in the *Ces3* deficient state (Fig. 2E). Consecutively,

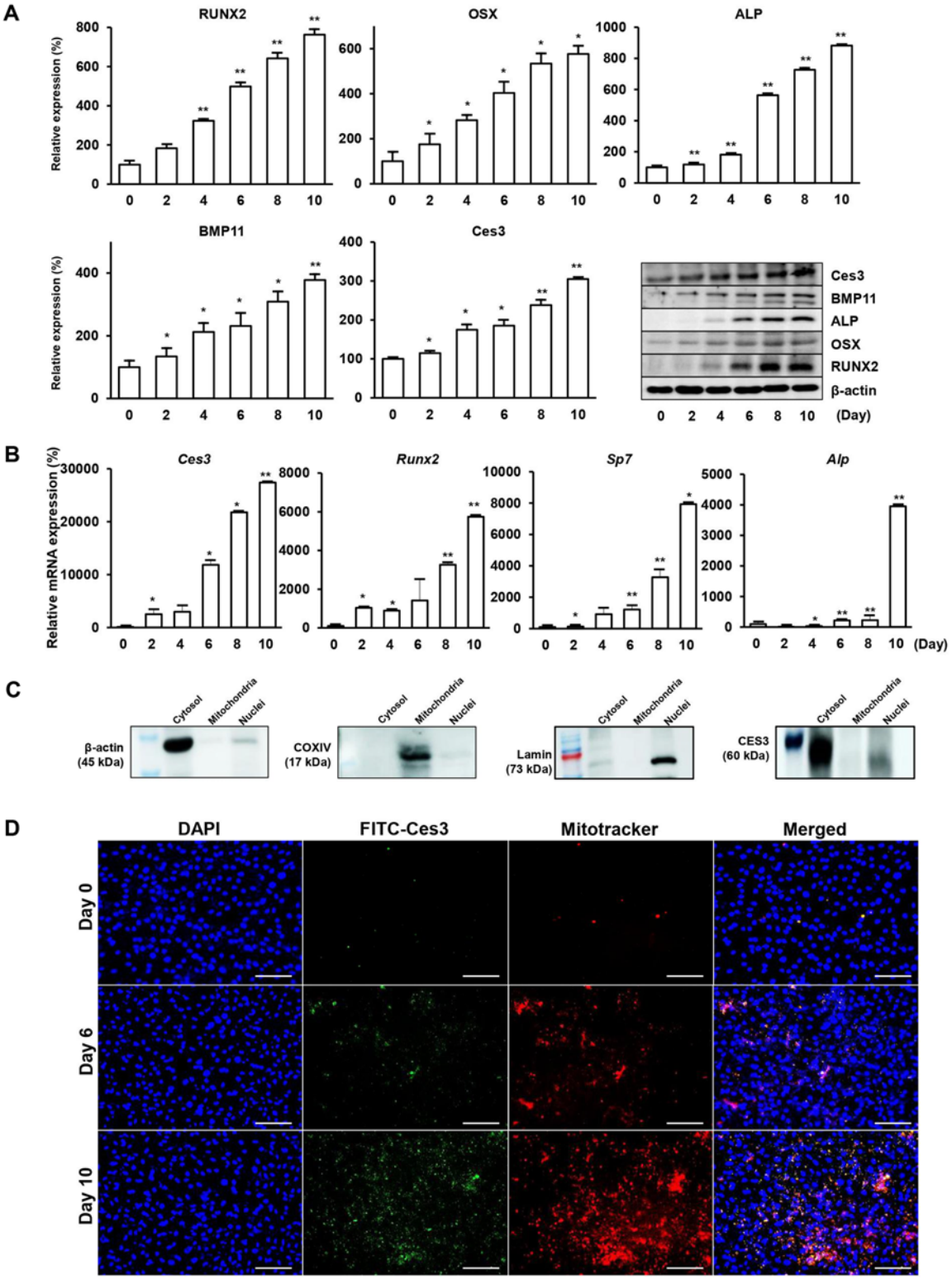

Fig. 1. Expression of Ces3 in osteoblasts. Day-dependent expression of osteoblast differentiation marker proteins and Ces3 from day 0 to day 10 (A) in MC-3T3-E1 cells. Day-dependent expression of genes encoding osteoblast differentiation between day 0 to day 10 (B) in MC-3T3-E1 cells. Presence of Ces3 protein in osteoblast cells samples after subcellular fractionation (with 5 μg protein loaded in each lane) (C). Immunocytochemistry for day-dependent expression of Ces3 protein in MC-3T3-E1 cells (D), where the immunofluorescent images were captured at X10 magnifications. All data are presented as the mean ± S.D., of three independent experiments and differences between groups were determined using ANNOVA by the Statistical Package of Social Science (SPSS, version 17.0; SPSS Inc., Chicago, IL, USA) program, followed by Tukey's post-hoc tests. Statistical significance s shown as $*p < 0.05$ or $**p < 0.01$.

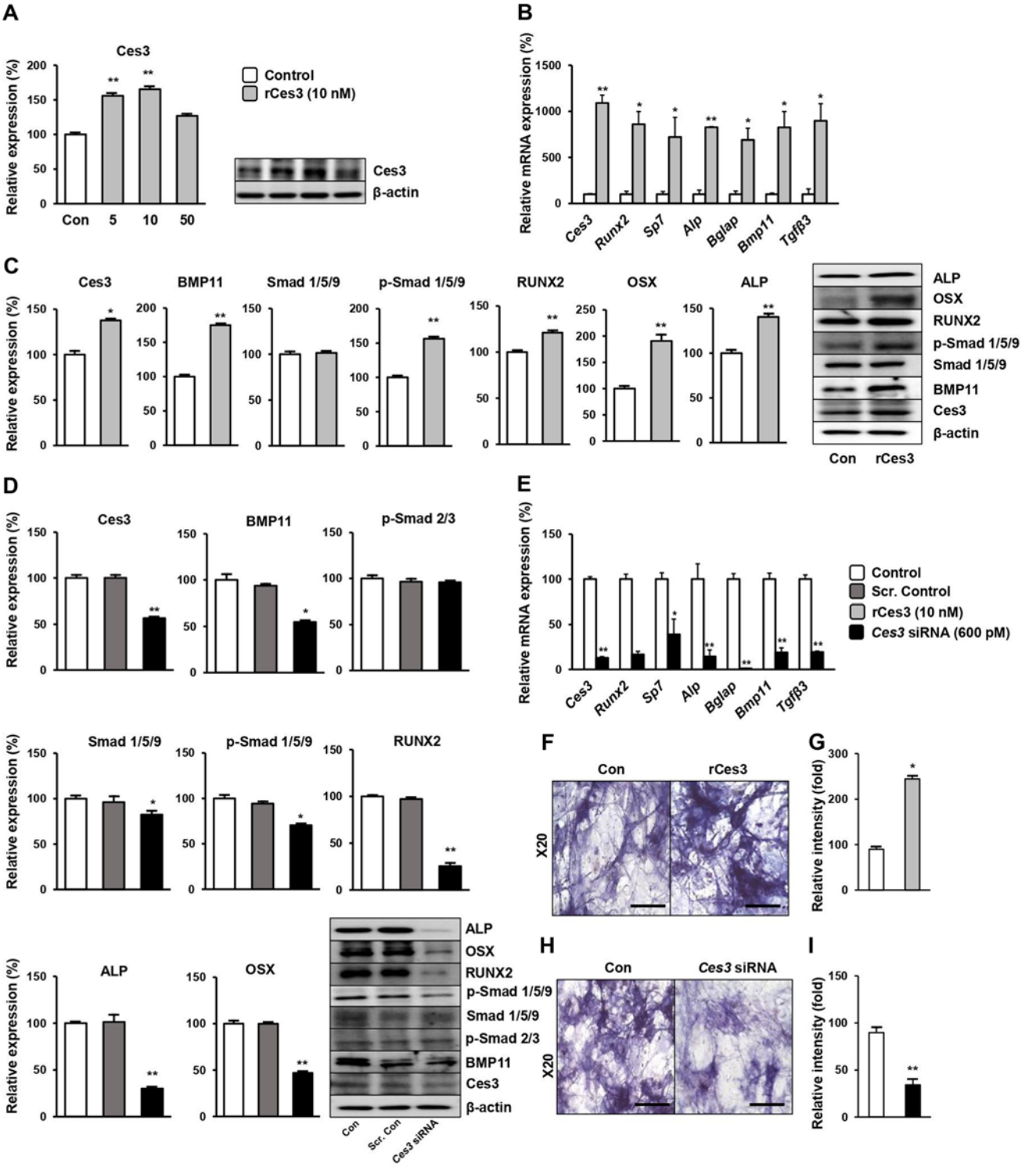

Fig. 2. Ces3 promotes proliferation of osteoblasts. MC-3T3-E1 osteoblasts treated with recombinant Ces3 (rCes3) in a concentration-dependent manner (A), optimizing a concentration of 10 nM rCes3 for further analysis of expressions for osteogenic genes (B) and proteins (C). Silencing of *Ces3* using transfection on MC-3T3-E1 cells with 600 pM siRNA to examine expressions of osteoblast differentiation marker proteins (D) and genes (E). Determination of bone cell mineralization by ALP staining for rCes3-treated MC-3T3-E1 cells (F) (X20 magnification; scale bar = 100 μm) and quantified fold changes (G). ALP staining for *Ces3*-deficient MC-3T3-E1 cells (H) (X20 magnification; scale bar = 100 μm) and quantified fold changes (I). All data are presented as the mean ± S.D., of three independent experiments and differences between groups were determined using ANNOVA by the Statistical Package of Social Science (SPSS, version 17.0; SPSS Inc., Chicago, IL, USA) program, followed by Tukey's post-hoc tests or Student's *t*-test. Statistical significance between control and rCes3-treated cells or *Ces3* siRNA-transfected cells is shown as $*p < 0.05$ or $**p < 0.01$.

we observed similar results for differentiating C3H10T1/2 stem cells (Fig. S2A and B). To further clarify the proliferation of the bone cells, we determined the initial mineralization for the differentiating osteoblasts by ALP staining after treatment with rCes3 (Fig. 2F), identifying increased ALP activity with a higher fold change (Fig. 2G). The deficiency of *Ces3* in MC-3T3-E1 cells showed reduced ALP activity determined by lower intensity of staining (Fig. 2H and I). Similar results for ALP staining were observed in differentiating stem cells (Fig. S1D and E and Fig. S2C and D).

3.3. BMP11 regulates osteoblast differentiation

As previously shown in Fig. 2, the expression of BMP11 protein resembles expression pattern of Ces3 in osteoblasts, due to which we investigated the role of BMP11 in differentiation of osteoblasts. As expected, deficiency of *Bmp11* showed reduced expression of Ces3 as well as other osteogenic marker proteins (Fig. 3A) and genes (Fig. 3B) in MC-3T3-E1 cells. In addition, the loss of *Bmp11* also decreased the ALP activity in bone cells (Fig. 3C and D). The results suggested an interconnection between BMP11 and Ces3 for regulatory mechanism of osteoblast differentiation.

3.4. BMP11 interacts with Ces3 for regulating osteodifferentiation

To examine the relation between Ces3 and BMP11 protein in osteoblasts we conducted the co-immunoprecipitation

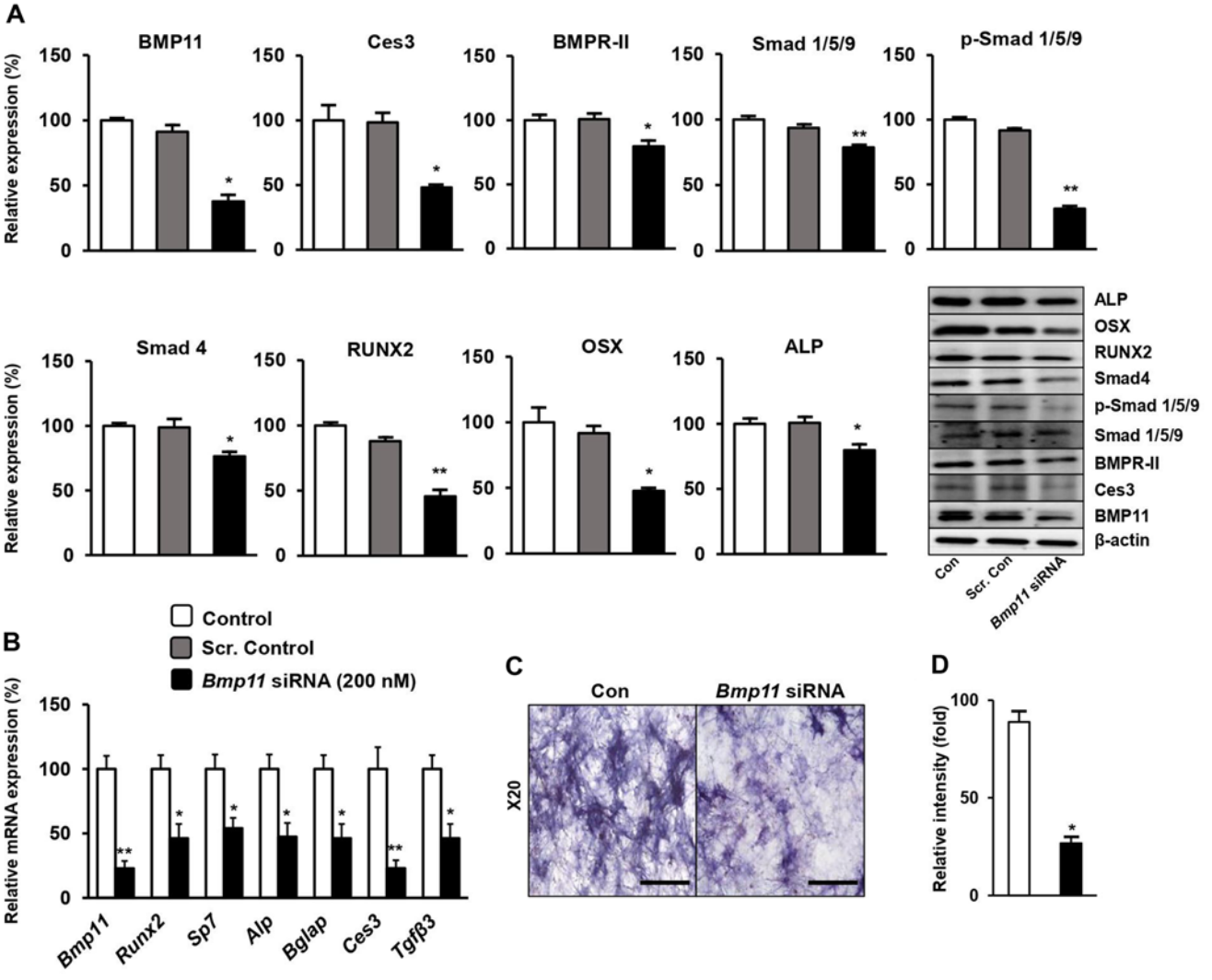

Fig. 3. Bmp11 regulates osteoblast differentiation. Silencing of *Bmp11* in MC-3T3-E1 cells by siRNA transfection at a dose of 200 nM to examine expressions of osteogenic differentiation marker proteins (A) and gene (B). Determination of bone cell mineralization by ALP staining for *Bmp11*-deficient osteoblasts (C) and quantified fold changes (D). All data are presented as the mean ± S.D., of three independent experiments and differences between groups were determined using ANNOVA by the Statistical Package of Social Science (SPSS, version 17.0; SPSS Inc., Chicago, IL, USA) program, followed by Tukey's post-hoc tests or Student's *t*-test. Statistical significance between control and *Bmp11* siRNA-transfected cells is shown as $*p < 0.05$ or $**p < 0.01$.

(Co-IP) analysis and confirmed the direct interaction between Ces3 and BMP11 in MC-3T3-E1 cells (Fig. 4A) and C3H10T1/2 cells (Fig. 4B), which displayed the expression of BMP11 protein in the rCes3-treated cells while Ces3 expression was identified in rBMP11-treated cells. Further, we used the other protein bands to identify

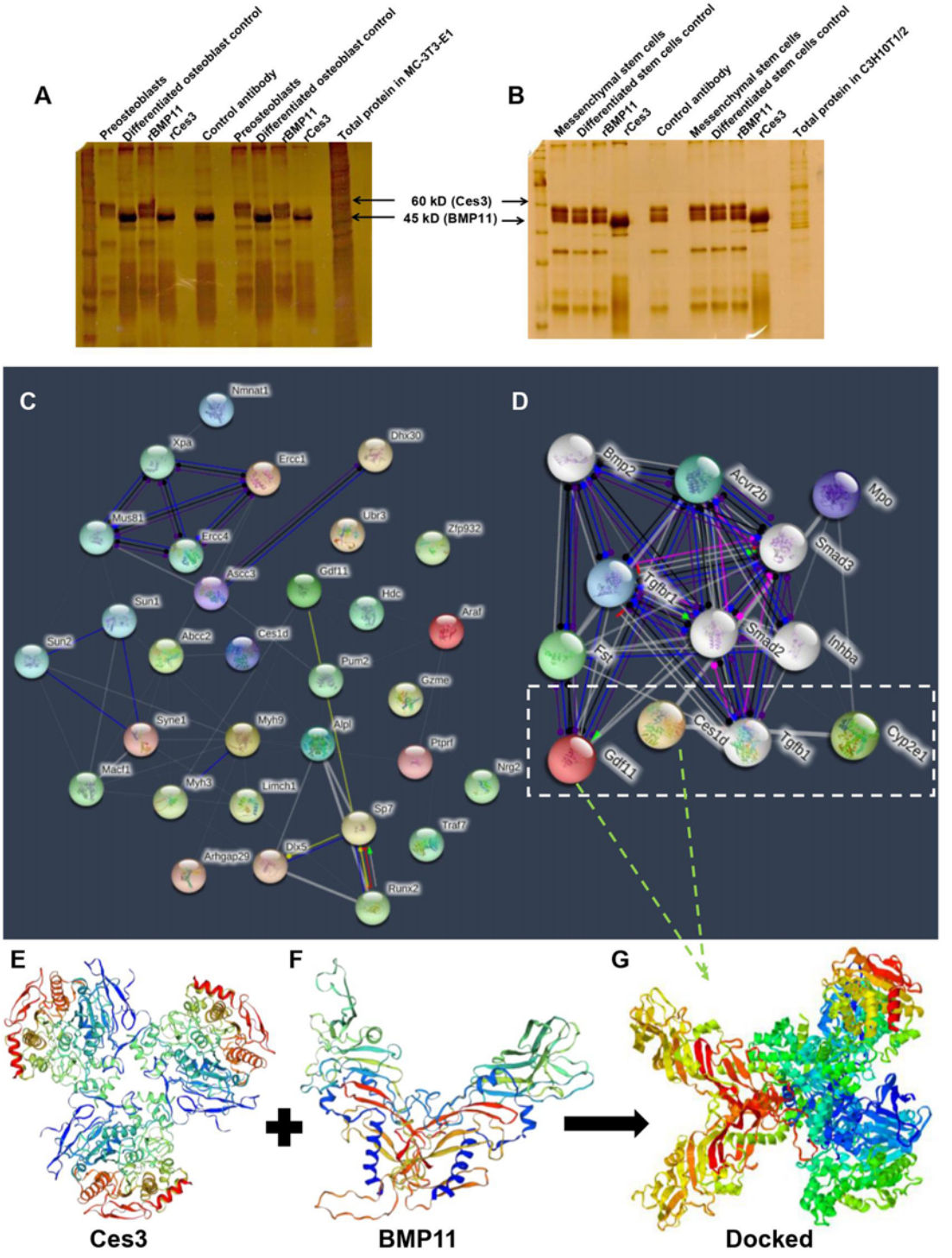

Fig. 4. BMP11 interacts with Ces3 for regulating osteodifferentiation. Co-IP analysis after treatment with rCes3 and rBMP11 to obtain silver-stained images for MC-3T3-E1 cells (A) and C3H10T1/2 mesenchymal stem cells (B). Predicted STRING network of Ces3 and BMP11 with various interacting proteins (displayed as gene names) identified by Co-IP analysis (C) and extended network with direct interaction of Ces3 and BMP11 (D). 3D structure of Ces3 (E) and BMP11 (F) bound together after molecular docking (G). Molecular docking generated by PatchDock software Beat 1.3 version.

Table 2. List of proteins identified in co-IP analysis and involved in STRING network

Protein name	Gene name	ID
Myosin-9	*Myh9*	Q8VDD5
LIM and calponin homology domains-containing protein 1	*Limch1*	D3YU59
Nesprin-1	*Syne1*	Q6ZWR6
ATP-dependent RNA helicase DHX30 (Fragment)	*Dhx30*	A0A0G2JGU3
Pro-neuregulin-2, membrane-bound isoform (Fragment)	*Nrg2*	D3YZR3
Canalicular multispecific organic anion transporter 1	*Abcc2*	Q3UNY3
Activating signal cointegrator 1 complex subunit 3 (Fragment)	*Ascc3*	A0A1W2P6I6
Protein-tyrosine-phosphatase (Fragment)	*Ptprf*	F6S1X8
Granzyme E	*Gzme*	P08884
Myosin-3	*Myh3*	P13541
Pumilio homolog 2 (Fragment)	*Pum2*	E9Q4Q6
Microtubule-actin cross-linking factor 1 (Fragment)	*Macf1*	F6XCT0
Non-specific serine/threonine protein kinase (Fragment)	*Araf*	B1AUN8
Zinc finger protein 932	*Zfp932*	D3Z5Z2
Histidine decarboxylase	*Hdc*	P23738
Zinc finger protein 431	*Znf431*	E9QAG8
Nicotinamide/nicotinic acid mononucleotide adenylyltransferase 1	*Nmnat1*	B0QZL2
DNA excision repair protein ERCC-1 (Fragment)	*Ercc1*	H3BJX2
E3 ubiquitin-protein ligase TRAF7	*Traf7*	Q922B6
Runt-related transcription factor 2	*Runx2*	Q08775
Transcription factor Sp7	*Sp7*	Q8VI67
Alkaline phosphatase, tissue-nonspecific isozyme	*Alpl*	P09242
Carboxylesterase 1D	*Ces1d*	Q8VCT4
Growth/differentiation factor 11	*Gdf11*	Q9Z1W4

the partner proteins interacting with Ces3 and BMP11 in osteoblasts by MALDI-TOF analysis (Table 2). Next, we utilized the identified proteins to build a network using STRING software for tracking the interactions between the proteins based on confidence rate, existing evidence as well as reported molecular interactions and generated a widely connected network displaying the genes involved in the network of Ces3 (represented as *Ces1d*) (Fig. 4C). In addition, we used only Ces3 and BMP11 as input to investigate the direct interaction and used an extended nodes setup to predict the linked proteins (Fig. 4D). Interestingly, BMP11 and Ces3 showed strong interaction pattern with Tgfβ1 and Cyp2e1 among the other proteins involved in the regulation of osteoblasts. Although we observed an interaction between Smad 2/3 protein in the extended network (Fig. 4D) with the BMP type 2 receptors, our results suggest the activation of p-Smad 1/5/9 protein only (Fig. 2). We also validated the results for interaction between Ces3 (Fig. 4E) and BMP11 (Fig. 4F) by molecular docking analysis, which resulted in a good binding score of -64.01 kcal/mol or -267.81 kJ/mol, and lowest conformational change as well as maximum surface area of binding (Fig. 4G). All the predictions up to top 10 binding confirmations are provided in Table S2. The *in-silico* analysis revealed a direct and a strong interaction between Ces3 and BMP11 which influences the growth and regulation of the osteoblasts.

3.5. Ces3 regulates differentiation of osteoblasts by activating Smad 1/5/9 pathway via ALK2 receptor

To identify the Ces3-mediated signaling pathway for osteogenic differentiation and other metabolic pathways, we investigated the BMP type 2 receptor, after observing no significant effect upon *Ces3*-lacking cells on p-Smad 2/3 (Fig. 2D), while the expression of p-Smad 1/5/9 reduced in *Ces3*-deficient cells and increased due to effect of rCes3. The gene expression for the osteoblast receptors were examined (*Acvr1*, *Acvr2a*, *Acvr2b*, and *Bmpr2*), and the expressions were highly reduced in *Ces3*-deficient cells (Fig. 5A), and showed increased expression in rCes3-treated cells (Fig. 5B). To elucidate the Smad pathway followed by Ces3, we treated the MC-3T3-E1 cells with rCes3 in the presence and absence of ALK2/3 antagonist, LDN193189 (1 μM) and determined the expression levels of osteogenic marker proteins (Fig. 5C). The Ces3-induced phosphorylation of Smad 1/5/9 was abolished subsequently by LDN193189 and exposure to the ALK2/3 antagonist suppressed the Ces3-induced osteogenic differentiation

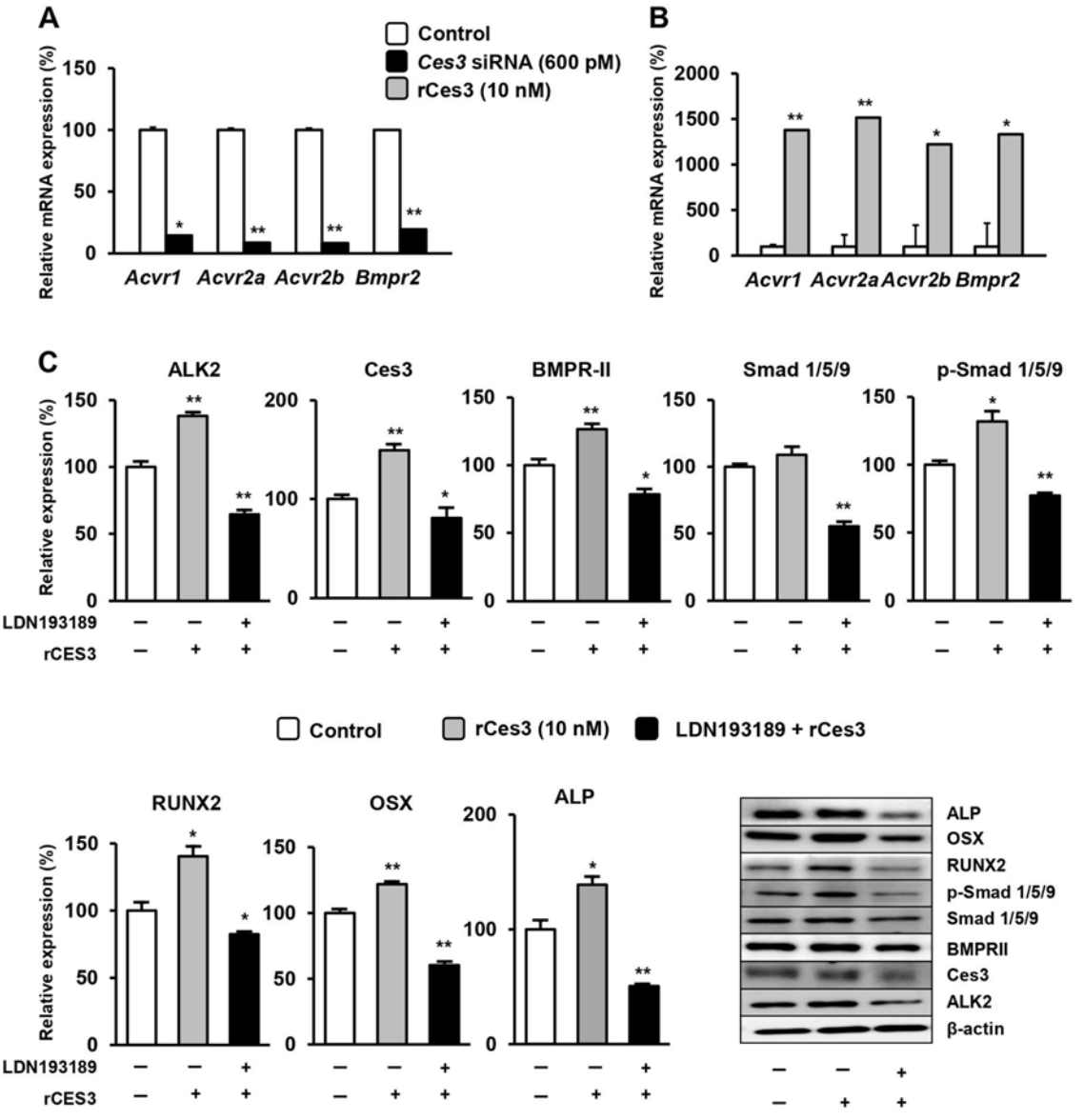

Fig. 5. Ces3 regulates differentiation of osteoblasts by activating Smad 1/5/9 pathway via ALK2 receptor. Quantified expression of BMP type 2 receptor genes in *Ces3*-deficient osteoblasts (A) and rCes3-treated cells (B). Expression of osteogenic differentiation protein markers after treatment of rCes3 in the presence or absence of ALK2/3 antagonist, LDN193189 (1 μM) in MC-3T3-E1 cells (C). All data are presented as the mean ± S.D., of three independent experiments and differences between groups were determined using ANNOVA by the Statistical Package of Social Science (SPSS, version 17.0; SPSS Inc., Chicago, IL, USA) program, followed by Tukey's post-hoc tests. Statistical significance between control and *Bmp11* siRNA-transfected cells is shown as $*p < 0.05$ or $**p < 0.01$.

marker proteins. This signified the involvement of Smad 1/5/9 in the Ces3-induced osteogenic differentiation in MC-3T3-E1 cells.

3.6. Ces3 regulates differentiation of MC-3T3-E1 cells along with BMP11 protein following Smad 1/5/9 signaling pathway

To interpret the canonical pathway driving the effects of Ces3 in osteoblasts, we examined the expression of signaling molecules and receptors (BMPRII, ALK2, Smad 1/5/9), and key osteogenic marker proteins (Runx2, Osx, and Alp) after treatment of rCes3 and silencing *Bmp11* or combination of both in MC-3T3-E1 cells (Fig. 6A). We observed an upregulation in expression of proteins only in rCes3-treated cells, while down regulation was seen only in *Bmp11*-deficient cells. Notably, all the proteins were highly upregulated in the *Bmp11*-deficient cells treated with rCes3. Consequently, we determined the expression of the same protein markers after silencing *Ces3* and treatment with rBMP11 together in the osteoblasts (Fig. 6B). Reduced

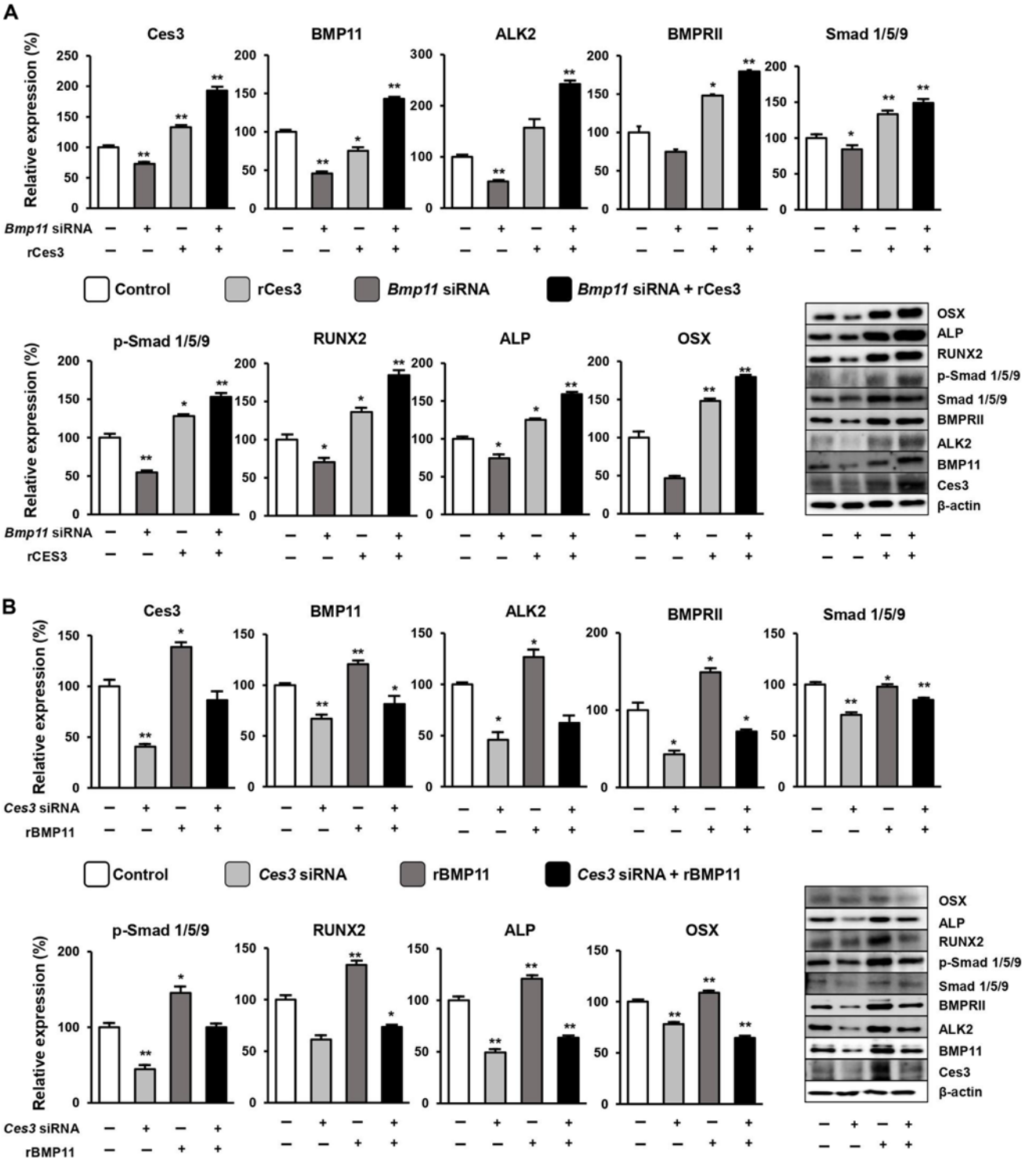

Fig. 6. Ces3 regulates differentiation of MC-3T3-E1 cells along with BMP11 protein following Smad 1/5/9 signaling pathway. Expression levels of key proteins involved in osteoblast differentiation and Smad1/5/9 signaling pathway after combined treatment of rCes3 and *Bmp11* silencing in MC-3T3-E1 cells (A). Expression levels of key proteins involved in osteoblast differentiation and Smad 1/5/9 signaling pathway after combined treatment of rBMP11 and *Ces3* silencing in MC-3T3-E1 cells (B). All data are presented as the mean ± S.D., of three independent experiments and differences between groups are determined by two-way ANOVA followed by Tukey's post-hoc tests using the Statistical Package of Social Science (SPSS, version 17.0; SPSS Inc, Chicago, IL, USA) program. Statistical significance between control and rCes3-treated or *Bmp11*-transfected cells and significance between control and rBMP11-treated or *Ces3*-transfected cells is shown as $*p < 0.05$ or $**p < 0.01$.

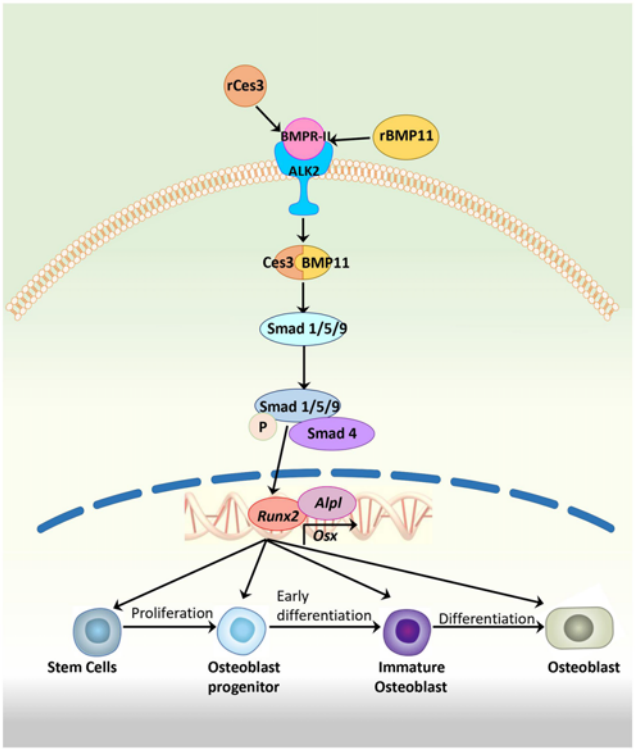

Fig. 7. Schematic diagram suggesting molecular mechanism of Ces3-BMP11 induced differentiation of osteoblast and mesenchymal stem cells.

expression of these proteins was observed only in *Ces3*-deficient cells, while upregulation of the proteins was markedly increased only in rBMP11-treated cells. In contrast to the previous observation (seen in Fig. 6A), none of the proteins showed any robust increase in the absence of *Ces3* after treatment with rBMP11. This indicates Ces3 as the upstream regulator of BMP11 in the activation of Smad 1/5/9 signaling pathway to promote osteoblast differentiation (Fig. 7).

4. Discussion

Ces3 is a well-known lipase widely distributed in white adipocytes [23,38], and contributes to thermogenesis by activating browning mechanism in white fat [33,30]. However, the role of Ces3 in osteoblasts is largely unknown. Although a recent study reported expression of *Ces3* gene in the skeletal muscle [16], to the best of our knowledge, Ces3 expression in osteoblasts has never been reported earlier. In this study, we not only identified Ces3 as a major protein expressed in osteoblasts (MC-3T3-E1) and differentiating stem cells (MC-3T3-E1) into osteoblast progeny, we also determined the physiological functions of Ces3 in promoting osteogenic differentiation in both these cells.

With respect to bone-adipose axis, earlier research has elucidated the impact of body weight on bone density and the role of metabolic enzymes produced in bone cells to regulate lipid metabolism [2,39]. Several studies have regarded the differentiation and proliferation of preosteoblasts as a complex but crucial process for the mineralization of bone mass [40], carried out by the master transcriptional regulators in a three step process through the activation of Runx2 and Osx, followed by Tgfβ and ALP proteins [41,42]. From our previous study, we have established a successful method of inducing recombinant exogenous protein *in vitro* for studying the effects and functions of the overly expressed form of protein in the cells [39]. Accordingly, our data verified the activation of these genes and proteins in the presence of rCes3 and reduced in *Ces3* deficient osteoblasts. Although Ces3 is reported to be a positive regulator in promoting adipogenesis [43], conflicting reports also suggest down regulation of PPAR signaling in adipocytes by Ces3 [31,32]. Hence, the possible involvement of Ces3 in osteogenic proliferation cannot be ruled out. Moreover, the formation of multilayered nodular structures instead of a cell monolayer with ALP-positive stain in our study, displayed the strong osteogenic lineage of the stem cells after addition of exogenous Ces3, as described by Zhu *et al.* (2009) [44].

Our very recent studies portrayed the functional role of BMP11 as well Ces3 in regulating thermogenic activity of white adipocytes [15,33]. The current study also reveals a crosstalk between BMP11 and Ces3. BMP11 has been reported to inhibit formation of bone by activation of Smad 2/3 pathways in stem cells [45]. A previous study reported that BMP11 may be linked to fat mass and obesity-associated protein (FTO) and PPARγ axis leading to inhibition of bone formation [46]. In contrast, other foregoing studies have demonstrated the protective effect of BMP11 in osteoblastogenesis by inhibition of PPARγ [47] and its role in promoting osteogenesis [48]. The results of the current study suggest the positive role of BMP11 on osteoblast differentiation in cells with a relatable expression of Ces3.

The differentiation of osteoblasts is regulated by numerous factors interacting with BMPs, involving both canonical and non-canonical pathways converging at the gene *Runx2* for further control of transcription [49]. Most of the BMPs activate the Smad-dependent pathways, predominantly, either Smad 2/3 or Smad 1/5/9 [50]. Likewise, we observed that Ces3 could phosphorylate Smad 1/5/9, while failing to activate the phosphorylation of Smad 2/3 in osteoblasts. Reportedly, Smad 1/5/9 forms a complex with other Smad proteins to transcribe the expression of Runx2 for initiation of osteogenic genes [51,52], which is in line with our results.

Apart from this, BMPs bind with two different types of

receptors, namely BMP type I receptor (BMPR-I) and type II receptor (BMPR-II) [53] to activate the signaling pathways [54,55]. In our study, BMPR-II was activated upon induction of exogenous Ces3. However, data from another study suggested the activation of Smad pathways even after deletion of BMP type II receptor in mice models [56].

The network analysis in the current study predicted a widely distributed network of bone regulating proteins interacting with Ces3 and BMP11. Earlier reports demonstrated that some of these proteins, such as LIM and calponin homology domains-containing protein 1(LIMCH1) [57], nesprin [58], histidine decarboxylase [59], and microtubule-actin cross-linking factor 1 [60,61] take active part in the growth and differentiation of osteoblasts and mesenchymal stem cells. The other proteins included in our network comprised of some of the transcription factors and activators of osteoblast specific genes including various zinc finger proteins (*Zfp932* and *Znf431*) [62] as well as canalicular multispecific organic anion transporter 1 (OAT1) which were previously reported to play pivotal roles in bone development, growth, and maintenance [63] and showed a direct link with Ces3 in the network. Proteins such as granzyme E showed direct links with BMP11 in our network of osteoblast regulating genes. It has been reported earlier that one isoform of granzyme (granzyme B) promoted osteoblastic differentiation and calcification with upregulated expression in bones [64], while another isoform (granzyme A) was reported to induce inflammation in other cell types [65].

Another protein of interest in our network analysis is myosin. Myosin has been reported to promote osteoclastogenesis with bone resorbption [66], and an earlier study has reported the role of myosin in regulating osteoblast differentiation [67]. We have also identified protein tyrosine phosphatase (encoded by *Ptrf*) from our generated network with supporting evidence to suggest that this protein actively remodels bone by resorbing osteoclasts and thereby affects osteoblast regulation [68]. Other proteins of interest in our network are non-specific serine/threonine protein kinase which promotes osteoblast regulation [69] and nicotinamide/nicotinic acid mononucleotide adenylyltransferase 1 (encoded by *Nampt1*) which stimulates insulin receptors and various related responses, including glucose uptake, proliferation of osteoblasts and type I collagenase production [70]. Although controversial, the protein pumilio homolog 2 (PUM2) that is responsible for developing adipose lineage in stem cells and is upregulated during osteogenesis [71], showed a connection with E3 ubiquitin-protein ligase TRAF7 in our network. In contrast, an earlier report had demonstrated that TRAF7 played a role in regulation of osteoblast metabolism [72]. Our network analysis also detected certain proteins related to bone disorders such as activating signal cointegrator 1 complex subunit 3 (ASCC3) and DNA excision repair protein ERCC-1 [73,74]. However, further studies are required to investigate in-depth, the functional roles of these proteins, in relation to Ces3 and BMP11.

Taken together, the results of this study indicate the expression of Ces3 in osteoblasts and stem cells differentiating into osteoblast lineage with a direct interaction of BMP11 in the regulation of cell proliferation via BMP type II receptor by activating the Smad 1/5/9 signaling pathway. In addition, we identified various partner proteins of Ces3 and BMP11 involved in the metabolic network of osteoblasts. In conclusion, current data unveiled a previously unknown mechanism in the regulation of Ces3 and BMP11 in the bone-adipose axis, shedding light on Ces3 as a pharmacotherapeutic target to treat metabolic disorders.

Acknowledgements

This study was supported by a National Research Foundation of Korea (NRF) grant funded by the Korean Government (MSIT, No. 2019R1A2C2002163).

Author's Contributions

Study design: SM and JWY. Data collection, analysis and interpretation: SM. Drafting manuscript: JPP. Revising and supervision of the manuscript: JWY. All authors read and approved the final manuscript.

Conflict of Interest

The authors declare that they have no conflicts of interest associated with this study.

Ethics Statement

The cellular *in vitro* models used in this study were commercially available. We did not use any human or animal samples and therefore did not require approval from the Ethics Committee.

Data Availability

Data will be made available on reasonable request.

Abbreviations

Acvr1, gene encoding activin receptor-like kinase-2; ***Acvr1b***, gene encoding activin receptor type-1B; ***Acvr2a***, gene encoding activin receptor type-2A; ***Acvr2b***, gene encoding activin receptor type-2B; **ALK2**, activin receptor-like kinase-2; **ALP**, alkaline phosphatase; ***Bglap***, gene encoding osteocalcin; **BMP11/*Bmp11***, bone morphogenetic protein 11 / encoding gene; ***Bmpr2***, gene encoding bone morphogenetic protein receptor type 2; **BMPRII**, bone morphogenetic protein receptor type 2; **Ces3/*Ces3***, carboxylesterase 3 / encoding gene; **COXIV**, cytochrome oxidase IV; **GDF11**, growth differentiation factor-11; **Osx**, Osterix; **Runx2/*Runx2***, Runt-related transcription factor 2 / encoding gene; ***Sp7***, gene encoding osterix; ***Tgfβ3***, gene encoding transforming growth factor beta-3.

Electronic Supplementary Material (ESM)

The online version of this article (doi: 10.1007/s12257-021-0133-y) contains supplementary material, which is available to authorized users.

References

1. Gómez-Ambrosi, J., A. Rodríguez, V. Catalán, and G. Frühbeck (2008) The bone-adipose axis in obesity and weight loss. *Obes. Surg.* 18: 1134-1143.
2. Kushwaha, P., M. J. Wolfgang, and R. C. Riddle (2018) Fatty acid metabolism by the osteoblast. *Bone.* 115: 8-14.
3. Gong, K., B. Qu, D. Liao, D. Liu, C. Wang, J. Zhou, and X. Pan (2016) MiR-132 regulates osteogenic differentiation via down-regulating sirtuin1 in a peroxisome proliferator-activated receptor β/δ-dependent manner. *Biochem. Biophys. Res. Commun.* 478: 260-267.
4. Blair, H. C., Q. C. Larrouture, Y. Li, H. Lin, D. Beer-Stoltz, L. Liu, R. S. Tuan, L. J. Robinson, P. H. Schlesinger, and D. J. Nelson (2017) Osteoblast differentiation and bone matrix formation *in vivo* and *in vitro*. *Tissue Eng. Part B Rev.* 3: 268-280.
5. Savopoulos, C., C. Dokos, G. Kaiafa, and A. Hatzitolios (2011) Adipogenesis and osteoblastogenesis: trans-differentiation in the pathophysiology of bone disorders. *Hippokratia.* 15: 18-21.
6. Muruganandan, S., A. M. Ionescu, and C. J. Sinal (2020) At the crossroads of the adipocyte and osteoclast differentiation programs: future therapeutic perspectives. *Int. J. Mol. Sci.* 21: 2277.
7. Berendsen, A. D. and B. R. Olsen (2014) Osteoblast-adipocyte lineage plasticity in tissue development, maintenance and pathology. *Cell Mol. Life Sci.* 71: 493-49.
8. Javed, A. (2001) Runt homology domain transcription factors (Runx, Cbfa, and AML) mediate repression of the bone sialoprotein promoter: evidence for promoter context-dependent activity of Cbfa proteins. *Mol. Cell Biol.* 21: 2891-2905.
9. Zhang, C. (2010) Transcriptional regulation of bone formation by the osteoblast-specific transcription factor Osx. *J. Orthop. Surg. Res.* 5: 37.
10. Wang, R. N., J. Green, Z. Wang, Y. Deng, M. Qiao, M. Peabody, Q. Zhang, J. Ye, Z. Yan, S. Denduluri, O. Idowu, M. Li, C. Shen, A. Hu, R. C. Haydon, R. Kang, J. Mok, M. J. Lee, H. L. Luu, and L. L. Shi (2014) Bone morphogenetic protein (BMP) signaling in development and human diseases. *Genes Dis.* 1: 87-105.
11. Katagiri, T. and T. Watabe (2016) Bone morphogenetic proteins. *Cold Spring Harb. Perspect. Biol.* 8: a021899.
12. Zhang, Y. H., L. H. Pan, Y. Pang, J. X. Yang, M. J. Lv, F. Liu, X. F. Qu, X. X. Chen, H. J. Gong, D. Liu, and Y. Wei (2018) GDF11/BMP11 as a novel tumor marker for liver cancer. *Exp. Ther. Med.* 15: 3495-3500.
13. Sharma, D., S. Kosalge, and S. R. Dixit (2017) Influence of GDF-11 in aging process: an review. *PharmaTutor.* 5: 18-29.
14. Añón-Hidalgo, J., V. Catalán, A. Rodríguez, B. Ramírez, C. Silva, J. C. Galofré, J. Salvador, G. Frühbeck, and J. Gómez-Ambrosi (2019) Circulating GDF11 levels are decreased with age but are unchanged with obesity and type 2 diabetes. *Aging.* 11: 1733-1744.
15. Pham, H. G., S. Mukherjee, M. J. Choi, and J. W. Yun (2021) Bmp11 regulates thermogenesis in white and brown adipocytes. *Cell Biochem. Funct.* 39: 496-510.
16. Raichur, S., R. L. Fitzsimmons, S. A. Myers, M. A. Pearen, P. Lau, N. Erikson, S. M. Wang, and G. E. O. Muscat (2010) Identification and validation of the pathways and functions regulated by the orphan nuclear receptor, ROR alpha1, in skeletal muscle. *Nucleic Acids Res.* 38: 4296-4312.
17. Lian, J., R. Nelson, and R. Lehner (2018) Carboxylesterases in lipid metabolism: from mouse to human. *Protein Cell.* 9: 178-195.
18. Li, D. (2019) The impact of carboxylesterases in drug metabolism and pharmacokinetics. *Curr. Drug Metab.* 20: 91-102.
19. Wang, X., N. Rida, J. Shi, A. H. Wu, B. E. Bleske, and H. J. Zhu (2017) A comprehensive functional assessment of carboxylesterase 1 nonsynonymous polymorphisms. *Drug Metab. Dispos.* 45: 1149-1155.
20. Laizure, S. C., V. Herring, Z. Hu, K. Witbrodt, and R. B. Parker (2013) The role of human carboxylesterases in drug metabolism: have we overlooked their importance? *Pharmacotherapy.* 33: 210-222.
21. Zhao, B., J. Bie, J. Wang, S. A. Marqueen, and S. Ghosh (2012) Identification of a novel intracellular cholesteryl ester hydrolase (carboxylesterase 3) in human macrophages: compensatory increase in its expression after carboxylesterase 1 silencing. *Am. J. Physiol. Cell Physiol.* 303: C427-C435.
22. Tanaka, N., S. Takahashi, Z. Z. Fang, T. Matsubara, K. W. Krausz, A. Qu, and F. J. Gonzalez (2014) Role of white adipose lipolysis in the development of NASH induced by methionine- and choline-deficient diet. *Biochim. Biophys. Acta.* 1841: 1596-1607.
23. Soni, K. G., R. Lehners, P. Metalnikov, P. O'Donnell, M. Semache, W. Goas, K. Ashman, A. V. Pshezhetsky, and G. A. Mitchell (2004) Carboxylesterase 3 (EC 3.1.1.1) is a major adipocyte lipase. *J. Biol. Chem.* 279: 40683-40689.
24. Okazaki, H., M. Igarashi, M. Nishi, M. Tajima, M. Sekiya, S. Okazaki, N. Yahagi, K. Ohashi, K. Tsukamoto, M. Amemiya-Kudo, T. Matsuzaka, H. Shimano, N. Yamada, J. Aoki, R. Morikawa, Y. Takanezawa, H. Arai, R. Nagai, T. Kadowaki, J. I. Osuga, and S. Ishibashi (2006) Identification of a novel member of the carboxylesterase family that hydrolyzes triacylglycerol: a potential role in adipocyte lipolysis. *Diabetes.* 55: 2091-2097.
25. Ruby, M. A., J. Massart, D. M. Hunerdosse, M. Schönke, J. C. Correia, S. M. Louie, J. L. Ruas, E. Näslund, D. K. Nomura, and J. R. Zierath (2017) Human carboxylesterase 2 reverses obesity-induced diacylglycerol accumulation and glucose intolerance. *Cell Rep.* 18: 636-646.
26. Ross, M. K., T. M. Streit, and K. L. Herring (2010) Carboxylesterases: dual roles in lipid and pesticide metabolism. *J. Pestic Sci.* 35: 257-264.

27. Quiroga, A. D., L. Li, M. Trotzmuller, R. Nelson, S. D. Proctor, H. Kofeler, and R. Lehner (2012) Deficiency of carboxylesterase 1/esterase-x results in obesity, hepatic steatosis, and hyperlipidemia. *Hepatology.* 56: 2188-2198.
28. Dominguez, E., A. Galmozzi, J. W. Chang, K. L. Hsu, J. Pawlak, W. Li, C. Godio, J. Thomas, D. Partida, S. Niessen, P. E. O'Brien, A. P. Russell, M. J. Watt, D. K. Nomura, B. F. Cravatt, and E. Saez (2014) Integrated phenotypic and activity-based profiling links Ces3 to obesity and diabetes. *Nat. Chem. Biol*. 10: 113-121.
29. Lian, J., E. Wei, S. P. Wang, A. D. Quiroga, L. Li, A. D. Pardo, J. van der Veen, S. Sipione, G. A. Mitchell, and R. Lehner (2012) Liver specific inactivation of carboxylesterase 3/triacylglycerol hydrolase decreases blood lipids without causing severe steatosis in mice. *Hepatology.* 56: 2154-2162.
30. Yang, L., X. Li, H. Tang, Z. Gao, K. Zhang, and K. Sun (2019) A unique role of carboxylesterase 3 (Ces3) in β-adrenergic signaling-stimulated thermogenesis. *Diabetes.* 68: 1178-1196.
31. Chang, J., S. Oikawa, H. Iwahashi, E. Kitagawa, I. Takeuchi, M. Yuda, C. Aoki, Y. Yamada, G. Ichihara, M. Kato, and S. Ichihara (2014) Expression of proteins associated with adipocyte lipolysis was significantly changed in the adipose tissues of the obese spontaneously hypertensive/NDmcr-cp rat. *Diabetol. Metab. Syndr*. 6: 8.
32. Magnum, L. C., X. Hou, A. Borazjani, J. H. Lee, M. K. Ross, and J. A. Crow (2018) Silencing carboxylesterase 1 in human THP-1 macrophages perturbs genes regulated by PPARγ/RXR and RAR/RXR: down-regulation of CYP27A1-LXRα signaling. *Biochem. J.* 475: 621-642.
33. Mukherjee, S., M. Choi, and J. W. Yun (2019) Novel regulatory roles of carboxylesterase 3 in lipid metabolism and browning in 3T3-L1 white adipocytes. *Appl. Physiol. Nutr. Metab*. 44: 1089-1098.
34. Dimauro, I., T. Pearson, D. Caporossi, and M. J. Jackson (2012) A simple protocol for the subcellular fractionation of skeletal muscle cells and tissue. *BMC Res. Notes* 5: 513.
35. Bridges, D., L. Chang, I. J. Lodhi, N. A. Clark, and A. R. Saltiel (2012) TC10 is regulated by caveolin in 3T3-L1 adipocytes. *PLoS One*. 7: e42451.
36. Duhovny, D., R. Nussinov, and H. J. Wolfson (2002) Efficient unbound docking of rigid molecules. *Proceedings of the Second Workshop on Al- rithms in Bioinformatics.* September 17-21. Rome, Italy.
37. Zhang, C., G. Vasmatzis, J. L. Cornette, and C. DeLisi (1997) Determination of atomic desolvation energies from the structures of crystallized proteins. *J. Mol. Biol.* 267: 707-726.
38. Joo, J. I., T. S. Oh, D. H. Kim, D. K. Choi, X. Wang, J. W. Choi, and J. W. Yun (2011) Differential expression of adipose tissue proteins between obesity-susceptible and -resistant rats fed a high-fat diet. *Proteomics*. 11: 1429-1448.
39. Mukherjee, S., K. R. Aseer, and J. W. Yun (2020) Roles of macrophage colony stimulating factor in white and brown adipocytes. *Biotechnol. Bioprocess Eng.* 25: 29-38.
40. Hanna, H., L. M. Mir, and F. M. Andre (2018) *In vitro* osteoblastic differentiation of mesenchymal stem cells generates cell layers with distinct properties. *Stem Cell Res. Ther*. 9: 203.
41. Jensen, E. D., R. Gopalakrishnan, and J. J. Westendorf (2010) Regulation of gene expression in osteoblasts. *Biofactors*. 36: 25-32.
42. Jo, I., J. M. Lee., H. Suh., and H. Kim (2007) Bone tissue engineering using marrow stromal cells. *Biotechnol. Bioprocess Eng.* 12: 48-53.
43. Challa, T. D., L. G. Straub, M. Balaz, E. Kiehlmann, O. Donze, G. Rudofsky, J. Ukropec, B. Ukropcova, and C. Wolfrum (2015) Regulation of de novo adipocyte differentiation through cross talk between adipocytes and preadipocytes. *Diabetes.* 64: 4075-4087.
44. Zhu, M., E. Kohan, J. Bradley, M. Hedrick, P. Benhaim, and P. Zuk (2009) The effect of age on osteogenic, adipogenic and proliferative potential of female adipose-derived stem cells. *J. Tissue Eng. Regen. Med.* 3: 290-301.
45. Lu, Q., M. L. Tu, C. J. Li, L. Zhang, T. J. Jiang, T. Liu, and X. H. Luo (2016) GDF11 inhibits bone formation by activating Smad2/3 in bone marrow mesenchymal stem cells. *Calcif. Tissue Int*. 99: 500-509.
46. Shen, G. S., H. B. Zhou, H. Zhang, B. Chen, Z. P. Liu, Y. Yuan, X. Z. Zhou, and Y. J. Xu (2018) The GDF11-FTO-PPARγ axis controls the shift of osteoporotic MSC fate to adipocyte and inhibits bone formation during osteoporosis. *Biochim. Biophys. Acta. Mol. Basis Dis*. 1864: 3644-3654.
47. Zhang, Y., J. Shao, Z. Wang, T. Yang, S. Liu, Y. Liu, X. Fan, and W. Ye (2015) Growth differentiation factor 11 is a protective factor for osteoblastogenesis by targeting PPARgamma. *Gene.* 557: 209-214.
48. Suh, J., N. K. Kim, S. H. Lee, J. H. Eom, Y. Lee, J. C. Park, K. M. Woo, J. H. Baek, J. E. Kim, H. M. Ryoo, S. J. Lee, and Y. S. Lee (2020) GDF11 promotes osteogenesis as opposed to MSTN, and follistatin, a MSTN/GDF11 inhibitor, increases muscle mass but weakens bone. *Proc. Natl. Acad. Sci. USA.* 117: 4910-4920.
49. Chen, G., C. Deng, and Y. P. Li (2012) TGF-β and BMP signaling in osteoblast differentiation and bone formation. *Int. J. Biol. Sci*. 8: 272-288.
50. Wu, M., G. Chen, and Y. P. Li (2016) TGF-β and BMP signaling in osteoblast, skeletal development, and bone formation, homeostasis and disease. *Bone Res*. 4: 16009.
51. Lee, K. S., S. H. Hong, and S. C. Bae (2002) Both the Smad and p38 MAPK pathways play a crucial role in Runx2 expression following induction by transforming growth factor-β and bone morphogenetic protein. *Oncogene*. 21: 7156-7163.
52. Franceschi, R. T. and G. Xiao (2003) Regulation of the osteoblast-specific transcription factor, Runx2: responsiveness to multiple signal transduction pathways. *J. Cell. Biochem.* 88: 446-454.
53. Yamaguchi, A., K. Sakamoto, T. Minamizato, K. Katsube, and S. Nakanishi (2008) Regulation of osteoblast differentiation mediated by BMP, notch, and CCN3/NOV. *Jpn. Dent. Sci. Rev.* 44: 48-56.
54. Zhang, Y., Y. Wei, D. Liu, F. Liu, X. Li, L. Pan, Y. Pang, and D. Chen (2017) Role of growth differentiation factor 11 in development, physiology and disease. *Oncotarget*. 8: 81604-81616.
55. Liu, H., R. Zhang, D. Chen, B. O. Oyajobi, and M. Zhao (2012) Functional redundancy of type II BMP receptor and type IIB activin receptor in BMP2-induced osteoblast differentiation. *J. Cell. Physiol*. 227: 952-963.
56. Huntley, R., E. Jensen, R. Gopalakrishnan, and K. C. Mansky (2019) Bone morphogenetic proteins: their role in regulating osteoclast differentiation. *Bone Rep.* 10: 100207.
57. Leuderer, H. F., B. Shuting, and G. D. Longmore (2008) The LIM protein LIMD1 influences osteoblast differentiation and function. *Exp. Cell Res.* 314: 2884-2894.
58. Yang, W., H. Zheng, Y. Wang, F. Lian, Z. Hu, and S. Xue (2013) Nesprin-1 plays an important role in the proliferation and apoptosis of mesenchymal stem cells. *Int. J. Mol. Med*. 32: 805-812.
59. Fitzpatrick, L. A., E. Buzas, T. J. Gagne, A. Nagy, C. Horvath, V. Fererncz, A. Mester, B. Kari, M. Ruan, A. Falus, and J. Barsony (2003) Targeted deletion of histidine decarboxylase gene in mice increases bone formation and protects against ovariectomy-induced bone loss. *Proc. Natl. Acad. Sci. USA*. 100: 6027-6032.
60. Qui, X. W., X. L. Ma, X. Lin, F. Zhao, D. J. Li, Z. H. Chen, K. W. Zhang, R. Zhang, P. Wang, Y. Y. Xiao, Z. P. Miao, K. Dang, X. Y. Wu, and A. R. Qian (2020) Deficiency of Macf1 in osterix expressing cells decreases bone formation by Bmp2/Smad/Runx2 pathway. *J. Cell Mol. Med*. 24: 317-327.

61. Hu, L., P. Su, C. Yin, Y. Zhang, R. Li, K. Yan, Z. Chen, D. Li, G. Zhang, L. Wang, Z. Miao, A. Qian, and C. J. Xian (2018) Microtubule actin crosslinking factor 1 promotes osteoblast differentiation by promoting β-catenin/TCF1/Runx2 signaling axis. *J. Cell. Physiol*. 233: 1574-1584.
62. Huang, G. J., Z. He, and L. Ma (2012) ZFP932 suppresses cellular hedgehog response and Patched1 transcription. *Vitam. Horm*. 88: 309-332.
63. Imai, Y., M. Y. Youn, K. Ioune, I. Takada, A. Kouzmenko, and S. Kato (2013) Nuclear receptors in bone physiology and diseases. *Physiol. Rev.* 93: 481-523.
64. Mao, M., M. Zhang, A. Ge, X. Ge, R. Gu, C. Zhang, Y. Fu, J. Gao, X. Wang, Y. Liu, and D. Zhu (2018) Granzyme B deficiency promotes osteoblastic differentiation and calcification of vascular smooth muscle cells in hypoxic pulmonary hypertension. *Cell Death Dis*. 9: 221.
65. Van Daalen, K. R., J. F. Reijneveld, and N. Bovenschen (2020) Modulation of inflammation by extracellular granzyme A. *Front. Immunol*. 11: 931.
66. Lee, B. S. (2018) Myosins in osteoclast formation and function. *Biomolecules.* 8: 157.
67. Munson, S., Y. Wang, W. Chang, and D. D. Bikle (2019) Myosin 1a regulates osteoblast differentiation independent of intestinal calcium transport. *J. Endocr. Soc*. 3: 1993-2011.
68. Shalev, M. and A. Elson (2019) The roles of protein tyrosine phosphatases in bone-resorbing osteoclasts. *Biochim. Biophys. Acta Mol. Cell Res*. 1866: 114-123.
69. Lezcano, V., T. Bellido, L. I. Plotkin, R. Boland, and S. Morelli (2014) Osteoblastic protein tyrosine phosphatases inhibition and connexin 43 phosphorylation by alendronate. *Exp. Cell Res*. 324: 30-39.
70. Garten, A., S. Petzold, A. Korner, S. I. Imai, and W. Kiess (2009) Nampt: Linking NAD biology, metabolism and cancer. *Trends Endocrinol. Metab*. 20: 130-138.
71. Shigunov, P., J. S. Silveira, C. Kuligovski, A. M. de Aguiar, C. K. Rebelatto, J. A. Moutinho, P. S. Brofman, M. A. Krieger, S. Goldenberg, D. Munroe, A. Correa, and B. Dallagiovanna (2012) PUMILIO-2 is involved in the positive regulation of cellular proliferation in human adipose-derived stem cells. *Stem Cells Dev.* 21: 217-227.
72. Zhang, Q., H. Matsui, H. Horiuchi, X. Liang, and K. Sasaki (2016) A-Raf and C-Raf differentially regulate mechanobiological response of osteoblasts to guide mechanical stress-induced differentiation. *Biochem. Biophys. Res. Commun*. 476: 438-444.
73. Knierim, E., H. Hirata, N. I. Wolf, S. Morales-Gonzalez, G. Schottmann, Y. Tanaka, S. Rudnik-Schöneborn, M. Orgeur, K. Zerres, S. Vogt, A. van Riesen, E. Gill, F. Seifert, A. Zwirner, J. Kirschner, H. H. Goebel, C. Hubner, S. Stricker, D. Meierhofer, W. Stenzel, and M. Schuelke (2016) Mutations in subunits of the activating signal cointegrator 1 complex are associated with prenatal spinal muscular atrophy and congenital bone fractures. *Am. J. Hum. Genet*. 98: 473-389.
74. Chen, Q., K. Liu, A. R. Robinson, C. L. Clauson, H. C. Blair, P. D. Robbins, L. J. Niedernhofer, and H. Ouyang (2013) DNA damage drives accelerated bone aging via an NF-kB-dependent mechanism. *J. Bone Miner. Res.* 28: 1214-1228.